Binding of Charged Ligands to Macromolecules. Anomalous Salt Dependence

ARTICLE *in* THE JOURNAL OF PHYSICAL CHEMISTRY B · MARCH 2005

Impact Factor: 3.3 · DOI: 10.1021/jp049304o · Source: PubMed

3 AUTHORS, INCLUDING:

Fernando Luís Barroso da Silva
University of São Paulo
24 PUBLICATIONS **353** CITATIONS
SEE PROFILE

Sara Linse
Lund University
197 PUBLICATIONS **8,460** CITATIONS
SEE PROFILE

Binding of Charged Ligands to Macromolecules. Anomalous Salt Dependence

Fernando Luís B. da Silva,*,†,‡ Sara Linse,§ and Bo Jönsson†

Department of Theoretical Chemistry and Department of Biophysical Chemistry, Lund University, P.O. Box 124, S-221 00 Lund, Sweden, Departamento de Física e Química, Faculdade de Ciências Farmacêuticas de Ribeirão Preto, Av. do café, s/no., Universidade de São Paulo, 14040-903 Ribeirão Preto, SP, Brazil

Received: February 16, 2004; In Final Form: October 16, 2004

Although interactions in biological systems occur in the presence of a large number of charged species, the binding of charged ligands to different biomolecules is often analyzed in a simplified model focusing only upon the receptor, ligand, and added salt. Here we demonstrate that the presence of charged macromolecules can affect binding to the receptor in an unexpected way. Experimental studies of the binding of barium ions to the chelator 5,5′-dibromo-1,2-bis(*O*-amino-phenoxy)-ethane-*N*,*N*,*N*′,*N*′-tetraacetic acid in the presence of charged silica sols show that the binding affinity increases with added salt. The experimental findings are verified in Monte Carlo simulations using a dielectric continuum model with a uniform dielectric permittivity throughout the solution. The anomalous salt behavior is caused by a reduction of the chemical potential of the free ligand, which even in the absence of binding interacts strongly with the oppositely charged receptor. These results are also relevant for the interpretation of competition studies often used in the case of strong ligand binding.

Biological systems always contain charged molecules, some of which are highly charged. The DNA molecule is a classical example, and the driving force for binding of different proteins to DNA has a large electrostatic component.[1,2] Since the early work of Linderstrøm-Lang,[3] and the classical paper of Tanford and Kirkwood,[4] electrostatic interactions have been the focus of many studies.[5−11] A particularly interesting problem is the binding of small charged ligands to proteins or DNA. The ligand could be a proton, a metal ion, a charged substrate, a polyelectrolyte, or another macromolecule like the *lac* repressor in the context of DNA.[12−17]

Theoretical studies of electrostatic interactions were initially performed within the framework of Debye−Hückel theory. That is the case, for instance, of the Tanford and Kirkwood (TK) model.[4] One limitation of such models is that closed form analytical solutions are only available for simple geometric configurations (usually spherical). Recently, with the advent of fast computers and improvements in the numerical algorithms, it has become possible to solve the TK model numerically for arbitrary molecular shapes and within the nonlinear Poisson−Boltzmann theory in substitution to the linear approximation of the Debye−Hückel theory.[18] Variants of this approach have been applied routinely to electrostatic interactions in biochemical systems.[7,10,19−23] All these procedures give approximate solutions for the given effective Hamiltonian of the system, but exact solutions can be obtained by numerical simulations using either Monte Carlo (MC) or molecular dynamics calculations.[8,24]

In the studies mentioned so far[4,7,8,10,19,20,22,23,25] the system has contained a further simplification: the calculations have only included *one* single charged macromolecule plus a simple electrolyte [Figure 1b]. A real system, in vivo, not only contains one type of charged aggregate and one single ligand but also consists of many charged molecules. In a cell, or in an

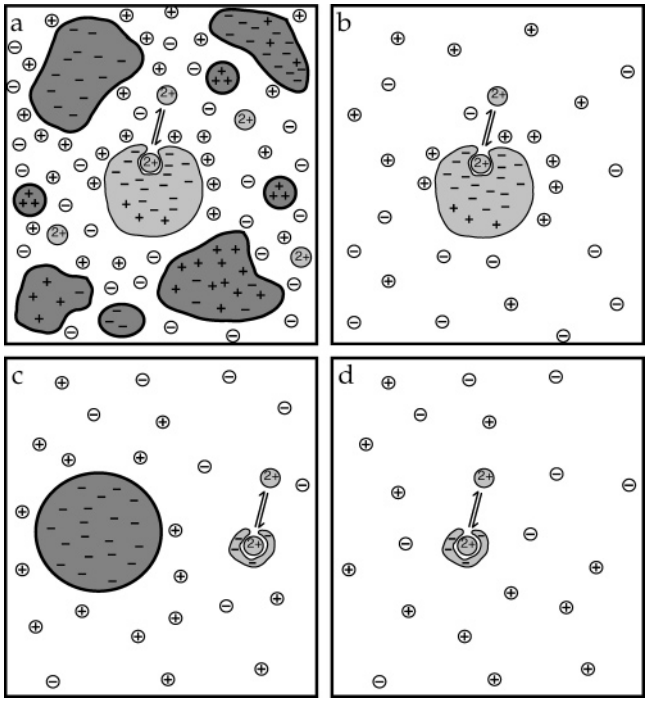

Figure 1. (a) Schematic picture of a complex cellular solution containing a variety of macromolecules as well as a simple salt. (b) An idealized picture for the binding of a divalent ligand to a protein. In this work we have studied ion binding to a model receptor, a chelator, in the presence (c) and absence (d) of inert charged particles. (For simplicity the chelator is treated as a spherical particle in the simulations.)

* Author responsible for correspondence. Phone: +55 (16) 602 4219 (direct) and +55 (16) 602 4222 (secretary). Fax: +55 (16) 633 2960.
† Department of Theoretical Chemistry, Lund University.
‡ Universidade de São Paulo.
§ Department of Biophysical Chemistry, Lund University.

10.1021/jp049304o CCC: $30.25
Published on Web 01/13/2005

extracellular environment, a charged protein with a specific binding site for a charged ligand is present in a solution of counterions and many other charged particles and electrolytes [Figure 1a]. This means that there are many electrostatic contributions to the net affinity between the protein and ligand. The charges on the protein may be of the same or opposite sign as the ligand and may be negative or positive determinants of the affinity. Screening effects may arise from the protein, ligand, counterions, and all other charged species in the solution. We attempt to investigate part of this complex system by comparing ligand binding affinities for a specific model receptor in the presence and absence of a charged macromolecule. An ideal macromolecule for these experiments is highly charged but is otherwise inert and does not interfere with the receptor or ligand through direct interactions. Silica sols fulfill all these requirements. The ideal model receptor−ligand system should have a significant electrostatic contribution to the binding affinity, should contain only one binding site, and should give a clear spectroscopic difference between free and bound forms. A small organic chelator for metal ions is a good candidate. The metal ion of choice must bind with an easily measurable affinity at all experimental conditions.

Hence, in this communication we present experimental results for the Ba^{2+} affinity of a small metal ion chelator (5,5′-dibromo-1,2-bis(*O*-amino-phenoxy)-ethane-*N*,*N*,*N*′,*N*′-tetraacetic acid = 5,5′-Br_2BAPTA) in the presence [Figure 1c] or absence [Figure 1d] of negatively charged silica sol particles at different KCl concentrations. In the combined case of chelator and silica sol, the binding process occurs in the presence of two types of charged molecules, leading to anomalous salt effects. The theoretical description of the process, using MC simulations, is straightforward and provides a direct explanation of the experimental findings in terms of the excess chemical potential (or activity factor) for the free barium ions.

Calcium signaling and buffer proteins bind calcium ions with a range of affinities, and the dissociation constants vary from millimolar to nanomolar depending on the location and function. It is often straighforward to quantitate the lower ($\log K = 2-6$) affinities in a direct experiment, using for example optical or NMR spectroscopy. However, the stronger sites ($\log K > 6$) are not amenable to such studies, simply because it is difficult to deplete buffers from calcium to sub-micromolar levels. To circumvent this problem it is common to use competition experiments in which the protein competes for calcium with a chelator with known affinity, and the binding to either the protein or the chelator is spectroscopically monitored. Alternatively, a large amount of chelator is used to buffer the free Ca^{2+} concentration, and the saturation level of the protein is monitored using spectroscopy. Although the competition experiments are generally thought of as giving high precision and low accuracy, as a result of possible errors in the affinity for the chelator, the present simulation highlights additional overlooked problems. If the protein is charged, and calcium binding proteins are often highly negatively charged, the calcium affinity for the chelator is affected in a similar way as demonstrated using the silica sols.

I. Experiments

Salt shifts for the binding of barium to 5,5′-Br_2BAPTA were studied in the presence and absence of silica particles. In terms of a chemical equilibrium we have

$$\mathrm{Ch} + \mathrm{Ba}^{2+} \overset{K_A}{\rightleftharpoons} \mathrm{ChBa}^{2} \quad \text{(Scheme A)} \tag{1}$$

Barium was chosen because its affinity for the chelator (Ch) is in a suitable range for direct measurements under all conditions of the present study. The chelator solution (2.1 mL) was titrated with $BaCl_2$ stock solution (5 μL of 3 or 10 mM $BaCl_2$), and binding was monitored by the absorbance at 263 nm. All solutions were in 2 mM Tris-HCl, pH 7.5, containing 0, 1, 2.5, 10, 25, 50, or 100 mM KCl. The chelator solution contained either 0 or 44 μM silical sol particles, while the $BaCl_2$ stock solutions were free from both chelator and silica sol. The chelator 5,5′-Br_2BAPTA was from Molecular Probes, and the silica sol used was Kromasol SO 0051 obtained from Eka Nobel. The average sol radius was 45 Å. All other chemicals were of the highest grade commercially available.

The (apparent) equilibrium Ba^{2+}-binding constant, K_A, was obtained by least-squares fitting to the absorbance as a function of total Ba^{2+} concentration, by minimizing the error square sum,

$$\sum_{i=0}^{N} (A_i^{\mathrm{calc}} - A_i^{\mathrm{obs}})^2 \tag{2}$$

where the sum runs over the $N + 1$ data points in the titration. The calculated absorbance, A_i^{calc}, at each titration point was obtained as

$$A_i^{\mathrm{calc}} = \left[\frac{(A_{\mathrm{Ba}} - A_{\mathrm{free}})[\mathrm{Ba}^{2+}]_i}{[\mathrm{Ba}^{2+}]_i + K_A^{-1}} + A_{\mathrm{free}} \right] \frac{V_0}{V_i} \tag{3}$$

where V_i and V_0 are the total volumes at titration point i and before adding the first $BaCl_2$ aliquot, respectively. A_{Ba} and A_{free} are the absorbances that the Ba−chelator complex and free chelator, respectively, would have at the initial chelator concentration. The free Ba^{2+} concentration, $[Ba^{2+}]_i$, was calculated as

$$[\mathrm{Ba}^{2+}]_i = -\frac{K_A^{-1} + [\mathrm{Ch}]_i^{\mathrm{tot}} - [\mathrm{Ba}^{2+}]_i^{\mathrm{tot}}}{2} + \left\{ \left(\frac{K_A^{-1} + [\mathrm{Ch}]_i^{\mathrm{tot}} - [\mathrm{Ba}^{2+}]_i^{\mathrm{tot}}}{2} \right)^2 + [\mathrm{Ba}^{2+}]_i^{\mathrm{tot}} K_A^{-1} \right\}^{1/2} \tag{4}$$

where $[\mathrm{Ch}]_i^{\mathrm{tot}}$ and $[\mathrm{Ba}^{2+}]_i^{\mathrm{tot}}$ are the total concentrations of chelator and barium, respectively, at point i corrected for the dilutions due to $BaCl_2$ additions. The initial chelator concentration, $[\mathrm{Ch}]_0$, was determined by withdrawing an aliquot of the solution and recording the absorbance at 239.5 nm in the presence of excess calcium (using $\epsilon = 4.2 \times 10^4\ \mathrm{M}^{-1}\ \mathrm{cm}^{-1}$). The adjustable parameters in the fit were K_A, A_{Ba}, and A_{free}.

II. Theory

Binding Constants. Consider a binding process where a small ligand (L) binds to a macromolecule (M) forming the complex ML,

$$\mathrm{M} + \mathrm{L} \rightleftharpoons \mathrm{ML} \tag{5}$$

At equilibrium $\Delta G = 0$, and when written in terms of the corresponding chemical potentials and activities, $\mu = \mu^0 + kT \ln a$, it reads

$$\mu_{\mathrm{ML}} - \mu_{\mathrm{M}} - \mu_{\mathrm{L}} = \mu_{\mathrm{ML}}^0 + kT \ln a_{\mathrm{ML}} - (\mu_{\mathrm{M}}^0 + kT \ln a_{\mathrm{M}} + \mu_{\mathrm{L}}^0 + kT \ln a_{\mathrm{L}}) = 0 \tag{6}$$

Introducing the *thermodynamic* binding constant, K, one obtains the familiar form

$$\Delta G^{o} = -kT \ln K = -kT \ln \frac{a_{ML}}{a_M a_L} \tag{7}$$

Many experiments involve the *stoichiometric* binding constant, K^s,

$$K = \frac{a_{ML}}{a_M a_L} = \frac{c_{ML}}{c_M c_L} \frac{\gamma_{ML}}{\gamma_A \gamma_L} = K^s \frac{\gamma_{ML}}{\gamma_M \gamma_L} \tag{8}$$

where the c's stand for concentrations and the γ's are activity coefficients. Because the thermodynamic binding constant is a true constant, any change in K^s is a measure of a change in the activity coefficients. It is convenient to choose a reference state with a corresponding stoichiometric binding constant, K^s_{ref}, and to measure any changes relative to this state. Let us also introduce the notation $\mu^{ex} = kT \ln \gamma$, which allows us to write the binding constant shift as

$$\Delta pK^s = -\log \frac{K^s}{K^s_{ref}} = \frac{\Delta\mu^{ex} - \Delta\mu^{ex}_{ref}}{kT \ln 10} \tag{9}$$

where $\Delta\mu^{ex} = \mu^{ex}_{ML} - \mu^{ex}_M - \mu^{ex}_L$ is the change in excess free energy for the binding process. In this work we will assume that the excess part is dominated by electrostatic interactions and that other contributions, including structural changes, solvation, and so forth, are either small or independent of added salt or other modifications of the electrostatic interactions. In the latter case they will cancel when calculating ΔpK^s. From a computational point of view it is advantageous to introduce the excess chemical potential of the bound ligand as $\mu^{ex}_B = \mu^{ex}_{ML} - \mu^{ex}_M$; hence, the electrostatic free energy difference can be expressed as

$$\Delta\mu^{ex} = \mu^{ex}_B - \mu^{ex}_F \tag{10}$$

where $\mu^{ex}_F = \mu^{ex}_L$ is the excess chemical potential of the free ligand, in our case Ba^{2+}. Thus, we will calculate the excess chemical potentials for varying salt concentrations, first in the system without the silica sols and then in the presence of the sol.

Model System. All systems were modeled within the cell model,[26,27] which has been used successfully in the past.[9,28] Both the chelator and the silica sol were described by hard spheres of radii R_{Ch} and R_{Si}, respectively. For the sake of simplicity, atomic details of the molecules are neglected, and just a single charge Z_M located at the center of the molecule is considered. The subscript Ch refers to the chelator, ChBa to the chelator−barium complex, and Si to the silica particle. Depending on what system is studied, one of these particles is kept fixed at the center of the spherical cell with radius R_c. All the other species are free to move within the cell or are introduced as perturbations; see the following. A picture of a macromolecule in the cell is given in Figure 2. Free ions are described as hard spheres of radius R_i with a central charge Z_i. No explicit water molecules are considered, but the solvent enters the calculations by means of its static dielectric constant, ϵ_s.

In a dielectric continuum model like this, there is often a choice of how to treat the macromolecule interior. This is sometimes a controversial point.[29−32] Nevertheless, the presence of a dielectric interface has been demonstrated to give unphysical results when used to predict the effect of mutations on the calcium binding constant to calbindin.[33] Linearized Poisson−Boltzmann calculations have also shown that it is necessary to increase the protein dielectric constant to improve the agreement with experimental titration data for proteins.[10] Moreover, calculations performed with a uniform continuum model reproduce experimental data with quite acceptable accuracy.[8,24,34,35] Hence, we assume here that the interior of the macromolecules has the same dielectric constant as the solvent.

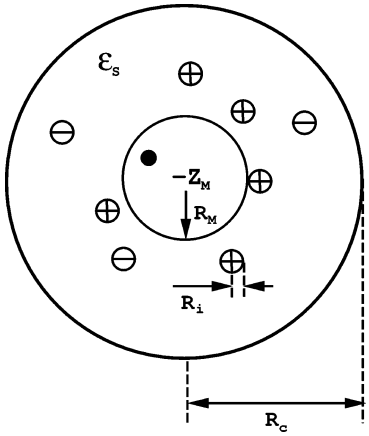

Figure 2. Schematic representation of the model system. A charged spherical macromolecule (e.g., a protein, a chelator, or a silica particle) in a spherical cell with radii R_M and R_C, respectively, is seen surrounded by free ions (radius R_i). The central charge has the valency Z_M. A binding site marked with a black dot is also shown.

Aggregate−aggregate interactions are partially taken into account by the definition of the macromolecular concentration defined by the cell radius R_C. The cell is always electroneutral, and the electrostatic interactions follow Coulomb's law. The pair potential including the short-range interaction is given by

$$u(r_{ij}) = \begin{cases} \infty & r_{ij} \le (R_i + R_j) \\ \dfrac{z_i z_j e^2}{4\pi\epsilon_0\epsilon_s r_{ij}} & \text{otherwise} \end{cases} \tag{11}$$

where e is the elementary charge, ϵ_0 is the vacuum permittivity, Z_i and Z_j denote the valency of particles i and j, respectively, r_{ij} is their separation, and R_i and R_j are their hard-core radii. If all mobile ions have the same size ($R_i = R_j$), which is our assumption here, the model is usually referred to as the "restricted primitive model".[36]

The total energy of the system for a given configuration $\mathbf{r}^N$ then becomes

$$U(\mathbf{r}^N) = \sum_{i=1}^{N_c+N_s} v^{ex}(r_i) + \frac{1}{2}\sum_{i=1}^{N}\sum_{j=1}^{N} u(r_{ij}) \tag{12}$$

$N = N_c + N_s + N_M$ is the total number of particles comprising N_c mobile counterions, N_s mobile added salt ions, and N_M number of macromolecules. The term $v^{ex}(r_i)$ is the imposed hard wall that defines the cell and macromolecule boundaries.

$$v^{ex}(r_i) = \begin{cases} 0 & (R_i + R_M) \le r_i \le R_C \\ \infty & \text{otherwise} \end{cases} \tag{13}$$

MC Simulations. The first set of simulations treated a salt solution plus a chelator fixed at the center of the cell. The binding site in the chelator was placed 3 Å from the chelator center. The radius of the chelator was 7 Å, and those of barium and the salt particles were 2.125 Å. In the second set of simulations a silica sol with a radius of $R_{Si} = 45$ Å was fixed at the center of the cell, and now the excess chemical potentials of barium, the chelator, and the chelator−barium complex were

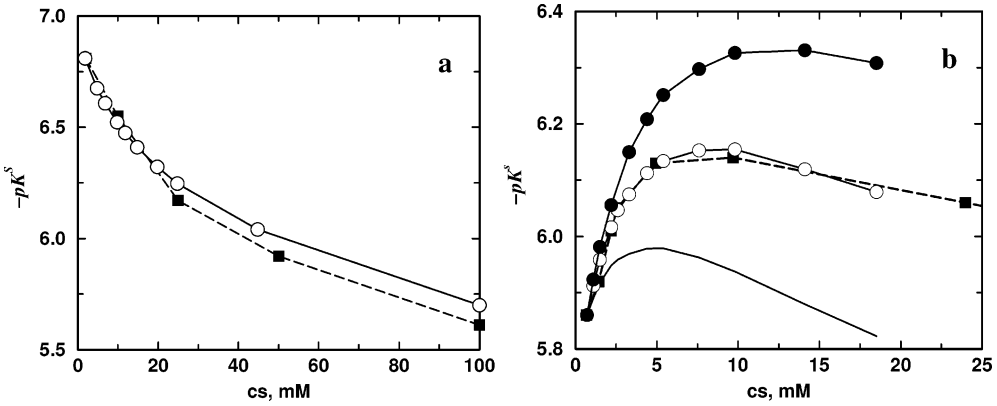

Figure 3. Binding constants for Ba^{2+} to 5,5′-Br_2BAPTA as a function of salt concentration in the (a) absence (left panel) and (b) presence (right panel) of silica particles at a concentration of 44 μM. Solid and dashed lines correspond to MC and experimental data, respectively. In the right panel, MC results for $Z_{Si} = -40$ are shown with no symbols, for $Z_{Si} = -50$ with open circles, and for $Z_{Si} = -60$ with filled circles. The experimental binding constants at 0.7 and 2.0 mM are taken as a reference for the theoretical calculations with and without the silica sol, respectively.

measured by the insertion technique. The radius of chelator−barium was assumed to be the same as that of the chelator itself, while the charge was reduced from $Z_{Ch} = -4$ to $Z_{ChBa} = -2$. The net charge of the silica particles is not known from experiments. Therefore, calculations were performed with values of Z_{Si} ranging from −10 to −60. Counterions and added salt were monovalent particles (symmetrical electrolyte 1:1) in all simulations.

The chelator concentration in the first set of simulations was $c_{Ch} = 0.2$ mM, and we note here that the binding constant of the chelator is only weakly affected by its concentration. The sol concentration in the second set of simulations was $c_{Si} = 44$ μM, and the salt concentration varied from 2 to 100 mM. In all cases, an appropriate number of counterions was added to obtain an electroneutral system.

The simulations were performed in the canonical (*NVT*) ensemble generated by the standard Metropolis MC algorithm.[37] After an initial equilibration, 100 000 simulation cycles were used to collected the final data. The excess free energy of any species can be obtained through a perturbation procedure, usually referred to as Widom's test particles technique.[38] To calculate μ_F^{ex} an appropriate test particle was inserted randomly over the simulation cell. The excess chemical potential is then calculated as

$$\beta\mu^{ex} = -\ln \langle \exp(-\beta \Delta U(\mathbf{r}^N, \mathbf{r}_T)) \rangle_0 \qquad (14)$$

where $\Delta U(\mathbf{r}^N, \mathbf{r}_T)$ is the interaction energy between the test particle at position $\mathbf{r}_T$ and all other particles in the system. The subscript $\langle ... \rangle_0$ indicates that the ensemble average is calculated over the unperturbed system, which has also been corrected for the finite system size.[39] That is, all types of insertions can be made in a single simulation. The chemical potential of the bound ligand is calculated simply by inserting a test particle into the binding site. Particles were inserted during the production phase with a probability of 20%. The temperature and static dielectric constant were fixed at 298 K and $\epsilon_s = 78.7$, respectively.

III. Results and Discussion

In the present study we have chosen a simple and well-defined system for studying electrostatic effects from charged particles that are present in a solution but are not directly involved in the interaction of interest. Silica particles were chosen as a substitute for charged biomolecules because they lack specific binding sites and functions that may interfere, yet their overall electrostatic properties resemble those of a charged macromolecule. A small organic chelator was taken as a model of a ligand binding site uncoupled from its protein matrix. Barium was used instead of calcium because the barium affinity for the chelator 5,5′-Br_2BAPTA was found to be in a range that is straighforward to quantitate from spectroscopic titrations at all conditions studied. The observed effects, however, should be general to the binding of any charged substrate to a specific binding site.

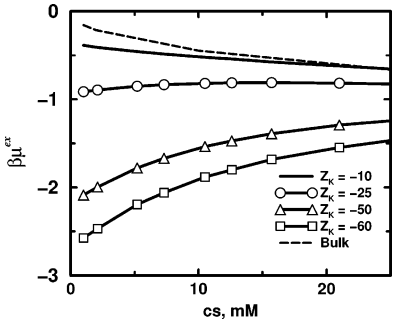

Figure 4. Reduced excess chemical potential for a free divalent cation in a 44 μM silica sol solution as function of added 1:1 electrolyte.

The barium affinity for the chelator was found to decrease monotonically with added salt [see Figure 3a], in a similar fashion as observed for many interactions between a charged ligand and a charged macromolecule studied in a simple buffer [cf. Figure 1d]. Strikingly different results were obtained when metal ion binding was studied in the presence of silica sols [Figure 1c]. At low salt, the barium affinity for the chelator is reduced by 1 order of magnitude because of the presence of the silica sol. In addition, the salt dependence is completely different. At low concentrations, salt additions lead to an increased barium affinity [see Figure 3b], while at higher concentrations the affinity decreases with added salt and approaches the values observed without sol particles, compare with Figure 3a. This corresponds to the situation depicted in Figure 1c.

The anomalous salt dependence observed in the presence of silica sol particles can be explained by the results of our theoretical calculations. The general behavior of the excess chemical potential for a free divalent cation as a function of the monovalent salt concentration in the presence of a highly negatively charged macromolecule is shown in Figure 4. At a low salt content, the free divalent cation is strongly affected by the macromolecule and the divalent cations are accumulated close to the sol. Figure 5 shows the simulated distribution function at two different salt concentrations, and one can in

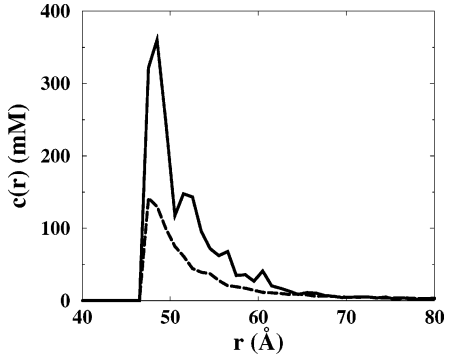

Figure 5. Radial distribution of divalent cations outside the negatively charged sol particle in a 1:1 salt solution. The salt concentrations are 0.17 mM (solid line) and 9.8 mM (dashed line), respectively.

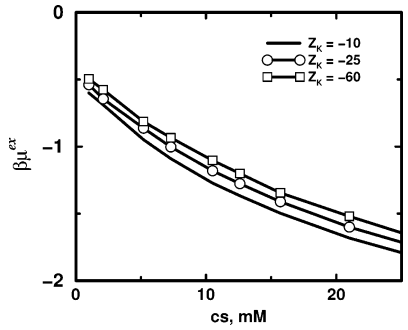

Figure 6. Reduced excess chemical potential for a free chelator ($Z_{Ch} = -4$) in a 44 μM silica sol solution as a function of monovalent salt concentration.

particular observe the strong accumulation of divalent cations at low salt concentration. The salt dependence for the chemical potential is completely opposite to what is found in a bulk solution, where the excess chemical potential initially always decreases with increasing salt concentration. In the presence of a highly charged macromolecule, we see the opposite and μ^{ex} is almost $3kT$ lower in the the dilute salt regime. At high electrolyte concentrations, the macromolecular charge becomes screened by salt particles and bulk behavior is approached. This effect has previously also been observed for the excess chemical potential of a free calcium in the presence of the protein calmodulin.[9]

The excess chemical potential of anions is less sensitive to the presence of the negatively charged macromolecule, as Figure 6 demonstrates. The chelator shows "normal" salt dependence, and the difference from the bulk value is only a few tenths of a kT. The explanation is simply that equally charged ions will stay away from the macromolecule, while the oppositely charged ones will sample the low potential region close to the macromolecule leading to a much lower excess chemical potential, compare with eq 14.

A comparison of the experimental and simulated binding constants in the absence and presence of silica particles is displayed in Figure 3a. The MC simulation data are in agreement with the experimentally determined salt dependence in the absence of silica sols. The added salt screens the interaction between the chelator and the barium ion, and binding becomes less favorable. A completely different behavior is seen in the presence of a highly charged silica sol in the electrolyte solution, Figure 3b, which is also reproduced by the MC simulations. In this case the added electrolyte primarily screens the interaction between the silica sol and the barium ion, raising the chemical potential of the latter and facilitating the binding to the chelator. In fact, this is already apparent from Figure 4. At sufficiently high salt concentration the screening of the interaction between barium and the chelator will be of significant magnitude and the binding constant starts to decrease.

As mentioned initially, we do not know the sol charge. However, the anomalous salt effect is sensitive to the charge and concentration of sol particles and is amplified at high sol concentration[9] and high sol charge, Figure 3b. The best agreement with experiment is obtained when a sol charge of -50 is used. Given the experimental difficulties of measuring the sol charge, it is more appropriate to determine the sol charge from simulations, which give an estimate of $Z_{Si} = -50$.

If a macromolecule (M) binds a ligand very strongly, then it is often impossible to measure the binding constant directly. The problem is typically circumvented by performing a competition study. That is, the ligand is allowed to bind to an appropriate chelator in the absence of any other macromolecule (Scheme A). In a second experiment the competition for the ligand, for example, a barium ion, between the biomolecule and the chelator is studied

$$\mathrm{M} + \mathrm{ChBa} \overset{K_B}{\rightleftharpoons} \mathrm{MBa} + \mathrm{Ch} \quad \text{(Scheme B)} \tag{15}$$

The standard way to calculate the binding constant for the process,

$$\mathrm{M} + \mathrm{Ba}^{2+} \overset{K_C}{\rightleftharpoons} \mathrm{MBa} \quad \text{(Scheme C)} \tag{16}$$

is by combining Schemes A and B, that is, $K_C = K_A K_B$. This is true for the thermodynamic binding constant but not for the stoichiometric one,

$$K_C^{\,s} \neq K_A^s K_B^s \tag{17}$$

which the silica sol experiment clearly shows. The presence of a macromolecule with a high charge opposite to the ligand will substantially reduce the excess chemical potential of the free ligand μ_F^{ex}. The excess chemical potentials of the other species are less affected and will approximately cancel.

In the competition experiment, K_A^s is assumed to have the same value as in the absence of macromolecules. This means that μ_F^{ex} is overestimated and the value obtained for K_C^s, calculated as $K_A^s K_B^s$, will be higher than in the direct experiment. Figure 7 shows how the binding constants for the two different routes vary with salt concentration. For low protein charges, the difference is negligible, but for more highly charged molecules, it becomes substantial. The system with $Z_M = -25$ corresponds roughly to the calcium binding protein calmodulin,[40] and in that case, the difference in Figure 7 is about one pK unit for the binding of *one* divalent ligand. Calmodulin binds *four* calcium ions; hence, the difference in the total binding constant between Scheme A + B and Scheme C increases to about four pK units! Note also that, at low salt concentration, the effect is only weakly dependent on protein concentration. However, because the ligand binding affinities for the chelator and protein are affected in a similar way, the results from the competition experiments may to a reasonable approximation be taken to reflect the situation at infinite dilution. While the direct experiment, Scheme C, is sensitive to protein concentration, the competition experiment is more or less independent of protein concentration. At very high protein or chelator concentrations additional complications might appear; for example, the chelator may bind to the protein.[41]

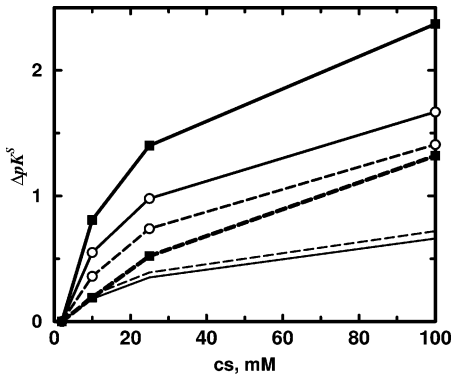

Figure 7. pK^s shifts as a function of salt concentration for different reaction schemes. Dashed and solid lines correspond to Schemes C and A + B, respectively. The concentration of macromolecule is 0.1 mM, the radius is 20 Å, and the binding site is located 15 Å from the center. Lines with no symbols are used for a macromolecule charge of $Z_M = -5$. Open circles and filled squares are used for macromolecule charges −15 and −25, respectively. The binding constant at 2.0 mM salt is taken as a reference. Theoretical numbers are significant to within 0.1 of a pK unit in this figure and Table 1.

TABLE 1: ΔpK^s upon Mutation[a]

mutation	Z_M	ΔpK^s_{A+B}	ΔpK^s_C	mutation	Z_M	ΔpK^s_{A+B}	ΔpK^s_C
single	−24	0.24	0.15	triple	−22	0.74	0.48
double	−23	0.49	0.29				

[a] The salt concentration is constant and equal to $c_s = 2$ mM, the protein concentration is 0.1 mM, and the "unmutated" protein with $Z_M = -25$ is taken as a reference. ΔpK^s_{A+B} is calculated as in a competition experiment following Schemes A and B, while ΔpK^s_C is calculated according to Scheme C.

The same artifact, but smaller in magnitude, is seen when the effect of a protein mutation is considered. Let us "mutate" the system with $Z_M = -25$ by replacing one, two, or three negatively charged amino acids with neutral analogues. In our computational scheme this corresponds to reducing Z_M to −24, −23, and −22, respectively. The result is shown in Table 1. Again, we find a significant difference between the direct determination of the binding constant and the one derived from the competition experiment, Scheme A + B.

IV. Conclusions

The binding of ions to a chelator has been analyzed in (i) simple electrolyte solution and (ii) in a salt with a highly charged inert macromolecule present. The macromolecule affects the chemical potential of other charged species and in particular those with an opposite charge. This can lead to an anomalous salt dependence. This is shown here using the negatively charged chelator 5,5′-Br_2BAPTA, as a model for a receptor site. The addition of salt *increases* the binding constant when a negatively charged macromolecule is present. This behavior was observed in experiments and was reproduced by MC simulations. The findings emphasize the fact that *all* charged species have to be included in the simulation of the interaction of charged species in complex mixtures. Furthermore, the good agreement with the experimental trends in binding gives further support to the use of a model with a uniform dielectric permittivity throughout the solution.

Acknowledgment. We thank Profs. Herman Berendsen and Torbjörn Åkesson for valuable comments on the manuscript. F.L.B.d.S. also acknowledges the *CNPq* and *FAPESP*/Brazil for the financial support during the development of this work.

References and Notes

(1) Spolar, R. S.; Record, M. T., Jr. Coupling of local folding to site-specific binding of proteins to DNA. *Science* **1994**, *263*, 777−784.

(2) Padmanabhan, S.; Zhang, W.; Capp, M. W.; Anderson, C. F.; Record, M. T., Jr. Binding of cationic (+4) alanine- and glycine- containing oligopeptides to double-stranded DNA: Thermodynamic analysis of effects of Coulombic interactions and α-helix induction. *Biochemistry* **1997**, *36*, 5193−5206.

(3) Linderstrøm-Lang, K. Om proteinstoffernes ionisation. *C. R. Trav. Lab. Carlsberg [Meddelelser fra Carlsberg Lab.]* **1924**, *15* (7), 1−28.

(4) Tanford, C.; Kirkwood, J. G. Theory of protein titration curves I. General equations for impenetrable spheres. *J. Am. Chem. Soc.* **1957**, *79*, 5333−5339.

(5) Perutz, M. F. Electrostatic effects in proteins. *Science* **1978**, *201*, 1187−1191.

(6) Sharp, K. A.; Honig, B. Electrostatic interactions in macromolecules: Theory and applications. *Annu. Rev. Biophys. Biophys. Chem.* **1990**, *19*, 301−332.

(7) Davis, M. E.; McCammon, J. A. Electrostatics in biomolecular structure and dynamics. *Chem. Rev.* **1990**, *90*, 509−521.

(8) Svensson, B.; Jönsson, B.; Woodward, C. E.; Linse, S. Ion binding properties of calbindin D_{9k} − A Monte Carlo simulation study. *Biochemistry* **1991**, *30*, 5209−5217.

(9) Svensson, B.; Jönsson, B.; Thulin, E.; Woodward, C. Binding of Ca^{2+} to calmodulin and its tryptic fragments: Theory and experiment. *Biochemistry* **1993**, *32*, 2828−2834.

(10) Juffer, A. H. Theoretical calculations of acid-dissociation constants of proteins. *Biochem. Cell Biol.* **1998**, *76*, 198−209.

(11) Warshel, A.; Papazyan, A. Electrostatic effects in macromolecules: fundamental concepts and pratical modeling. *Curr. Opin. Struct. Biol.* **1998**, *8*, 211−217.

(12) Poland, D. Ligand binding distributions in nucleic acids. *Biopolymers* **2001**, *58* (5), 477−490.

(13) Boroudjerdi, H.; Netz, R. R. Interactions between polylectrolyte-macroion complexes. *Eur. Phys. Lett.* **2003**, *64* (3), 413−419.

(14) Grosberg, A. Y.; Nguyen, T. T.; Shklovskii, B. I. Colloquium: The physics of charge inversion in chemical and biological systems. *Rev. Mod. Phys.* **2002**, *74*, 329−345.

(15) Vries, R. Monte Carlo simulations of flexible polyanions complexing with whey proteins at their isoelectric point. *J. Chem. Phys.* **2004**, *120* (7), 3475−3481.

(16) Yoshida, K.; Sokhakian, S.; Dubin, P. L. Binding of Polycarboxylic Acids to Cationic Mixed Micelles, Effects of Polymer Counterion Binding and Polyion Charge Distribution. *J. Colloid Interface Sci.* **1998**, *205*, 257−264.

(17) Doublier, J. L.; Garnier, C.; Renard, D.; Sanchez, C. Protein-polysaccharide interactions *Curr. Opin. Colloid Interface Sci.* **2000**, *5*, 202−214.

(18) Warwicker, J.; Watson, H. C. Calculation of the electric potential in the active site cleft due to α-helix dipoles. *J. Mol. Biol.* **1982**, *157*, 671−679.

(19) Bashford, D.; Karplus, M. pKa's of ionizable groups in proteins: Atomic detail from a continuum electrostatic model. *Biochemistry* **1990**, *29*, 10219−10225.

(20) Beroza, P.; Fredkin, D. R.; Okamura, M. Y.; Feher, G. Protonation of interacting residues in a protein by a Monte Carlo method: Application to lysozyme and the photosynthetic reaction center of *rhodobacter sphaeroides*. *Proc. Natl. Acad. Sci. U.S.A.* **1991**, *88*, 5804−5808.

(21) Juffer, A. H. On the Modelling of Solvent Mean Force Potentials − From Liquid Argon to Solvated Macromolecules. Ph.D. Thesis, Rijkuniversiteit Groningen, The Netherlands, 1993.

(22) Juffer, A. H.; Botta, E. F. F.; van Keulen, B. A. M.; van der Ploeg, A.; Berendsen, H. J. C. The electric potential of a macromolecule in a solvent: a fundamental approach. *J. Comput. Phys.* **1991**, *97*, 144−171.

(23) Warwicker, J. Simplified methods for pK_a and acid pH-dependent stability estimation in proteins: Removing dielectric and counterion boundaries. *Protein Sci.* **1999**, *8*, 418−425.

(24) Kesvatera, T.; Jönsson, B.; Thulin, E.; Linse, S. Measurement and modelling of sequence-specific pK_a values of Calbindin D_{9k}. *J. Mol. Biol.* **1999**, *259*, 828.

(25) Bashford, D.; Karplus, M.; Canters, G. W. Electrostatic effects of charge perturbations introduced by metal oxidation in proteins − a theoretical analysis. *J. Mol. Biol.* **1998**, *203*, 507−510.

(26) Hill, T. L. *Statistical Mechanics*; McGraw-Hill: New York, 1956.

(27) Marcus, R. A. Calculation of thermodynamic properties of polyelectrolytes. *J. Chem. Phys.* **1955**, *23*, 1057.

(28) Jönsson, B. The Thermodynamics of Ionic Amphiphilie-Water Systems − A Theoretical Analysis. Ph.D. Thesis, Lund University, Lund, Sweden, 1981.

(29) Harvey, S. C. Treatment of electrostatic effects in marcomolecular modeling. *Proteins: Struct., Funct., Genet.* **1989**, *5*, 78−92.

(30) Bashford, D. Electrostatic effects in biological molecules. *Curr. Opin. Struct. Biol.* **1991**, *1*, 175−184.

(31) Sharp, K. A. Electrostatic interactions in macromolecules. *Curr. Opin. Struct. Biol.* **1994**, *4*, 234−239.

(32) Warshel, A.; Åqvist, J. Electrostatic energy and macromolecular function. *Annu. Rev. Biophys. Biophys. Chem.* **1991**, *20*, 267−298.

(33) da Silva, F. L. B.; Jönsson, B.; Penfold, R. A critical investigation of the Tanford-Kirkwood scheme by means of Monte Carlo simulations. *Protein Sci.* **2001**, *10*, 1415−1425.

(34) Kesvatera, T.; Jönsson, B.; Thulin, E.; Linse, S. Binding of Ca^2 to calbindin D_{9k}: Structural stability and function at high salt concentration. *Biochemistry* **1996**, *33*, 14170−14176.

(35) Penfold, R.; Warwicker, J.; Jönsson, B. Electrostatic models for calcium binding proteins. *J. Phys. Chem. B* **1998**, *108*, 8599−8610.

(36) Levesque, D.; Weis, J. J.; Hansen, J. P. Simulation of classical fluids. In *Monte Carlo Methods in Statistical Physics*; Binder, K., Ed.; Springer-Verlag: Berlin, 1986; Vol. 5, pp 47−119.

(37) Frenkel, D.; Smit, B. *Understanding Molecular Simulation: From Algorithms to Applications*; Academic Press: San Diego, 1996.

(38) Widom, B. Some topics in the theory of fluids. *J. Chem. Phys.* **1963**, *39*, 2808−2812.

(39) Svensson, B. R.; Woodward, C. E. Widom's method for uniform and nonuniform electrolyte solutions. *Mol. Phys.* **1988**, *64*, 247−259.

(40) Vogel, H. J.; Calmodulin: a versatile calcium mediator protein. *Biochem. Cell Biol.* **1994**, *72*, 357−376.

(41) Chiancone, E.; Thulin, E.; Boff, A.; Forsén, S.; Brunor, M. Evidence for the interaction between the calcium indicator 1,2-Bis(o-aminophenoxy)ethane N,N,N′,N′-tetraacetic acid and calcium binding proteins. *J. Biol. Chem.* **1986**, *261*, 16306−16308.